ACS Sustainable Chemistry & Engineering

pubs.acs.org/journal/ascecg

Research Article

Cell Wall Chemical and Structural Changes of Wood by Steam Explosion to Increase Fungal Growth for Myco-Composite Production

Laura Figel,[#] Kyle Aguilar,[#] Isabelle Ziegler-Devin, Safwan Saker, Nicolas Brosse, and Arnaud Besserer*

Cite This: https://doi.org/10.1021/acssuschemeng.5c00929

Read Online

ACCESS | Metrics & More | Article Recommendations | Supporting Information

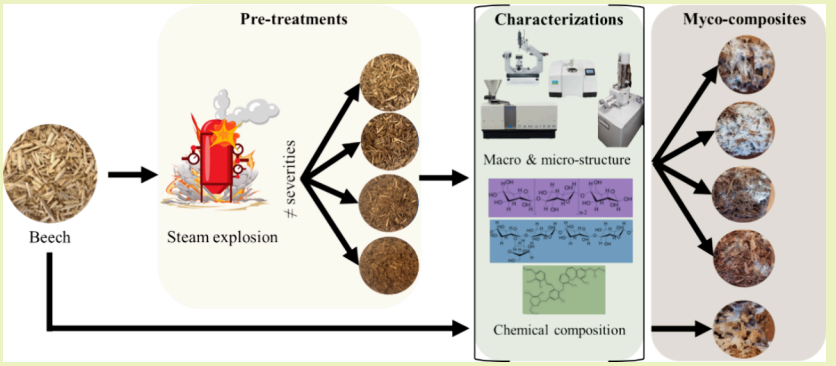

ABSTRACT: The production of myco-composites, sustainable materials formed by fungal growth through lignocellulosic substrates, requires efficient fungal colonization of the feedstock. This study highlights the potential of steam explosion (SE) as an effective pretreatment to enhance the bioavailability of beech wood components for myco-composite production. Wood samples were subjected to steam explosion under four different severities ($R_{0\ 3.36}$; $R_{0\ 3.65}$; $R_{0\ 3.94}$; $R_{0\ 4.24}$), and their chemical composition and microstructure were analyzed by dynamic image analysis, scanning electron microscopy, drop shape analysis, near-infrared spectroscopy, and anionic chromatography. By modifying the chemical composition and microstructure of wood particles, SE improves substrate accessibility for fungal colonization and generates a nutrient medium with minimal inhibitory compounds, promoting optimal fungal growth. Our findings reveal that *Trametes versicolor* exhibits its highest growth rate and larger hyphal diameters (1.3 vs 0.5 μm) on beech wood particles treated at intermediate severities ($R_{0\ 3.36–3.94}$) with growth rates increasing by 46% compared to condition $R_{0\ 4.24}$ and 138% compared to untreated beech. These results were correlated with a reduction in fine particles (0.7 vs 11.6% at $R_{0\ 4.24}$) and better water absorption (28 vs 5% at $R_{0\ 4.24}$). The myco-composite produced with $R_{0\ 3.65}$ showed 69% thickness recovery compared to 32% ($R_{0\ 3.36}$) and 41% ($R_{0\ 4.24}$). Fungal growth inhibition occurred at $R_0 > 3.7$, emphasizing the critical window for pretreatment severity. These results demonstrate the importance of substrate characterization in balancing digestibility and nutrient integrity, providing a pathway for the efficient and sustainable myco-composite production from wood and recalcitrant biomass.

KEYWORDS: *myco-composite, mycelium based material, pretreatment, steam explosion*

INTRODUCTION

For more than 30 years, major research efforts has been underway to overcome the recalcitrance of wood to the fermentative production of second-generation (2G) bioethanol. Various pretreatment technologies have been studied and optimized to break down the protective barrier of lignin and increase the accessibility of wood sugars to enzymes and yeasts, such as dilute acid pretreatment[1] or hot-compressed water pretreatment.[2] Among all the technologies studied in the literature, the steam explosion (SE) process is the most advanced pretreatment, even on an industrial scale.[3,4] In SE, the biomass is saturated with steam under high pressure (typically 8−20 bar) for a few minutes, and then the reactor is rapidly depressurized. This sudden pressure drop causes rapid water vaporization within the biomass, converting thermal energy into mechanical energy and resulting in the breakdown of the lignocellulosic structure.[5] The high-temperature cooking step combined with the quick depressurization results in substantial physical and chemical changes to the biomass, such

Received: February 3, 2025
Revised: April 23, 2025
Accepted: April 23, 2025

as partial hydrolysis of hemicelluloses and relocation of part of the lignin to the fiber surface.[5] These modifications make the lignocellulosic biomass more accessible to enzymes and fermentation for subsequent processes. Pretreatment costs and environmental impact have been evaluated through a number of research studies. When compared to traditional alternatives such as thermohydrolysis, dilute acid prehydrolysis, organosolv processes, and ionic liquid pretreatment, SE has been demonstrated to be more economical with a smaller carbon footprint.[6,7] As a result, SE is currently used on a large scale as a lignocellulose pretreatment in 2G cellulosic biorefineries.

Myco-composite is a sustainable material made by combining fungal mycelium with organic lignocellulosic materials.[8] The mycelium grows through the fibers, binding them together into a solid and durable structure. This process creates a natural, biodegradable composite that can be molded into various shapes and used as an alternative to conventional materials. Myco-composite is a promising eco-friendly material for a wide range of applications in packaging, construction, and even furniture. It offers a renewable, environmentally friendly option that reduces waste and carbon emissions.[9] In the context of the circular bioeconomy, myco-composites represent an innovative solution that aligns with principles of resource use efficiency and waste reduction.[10] Myco-composites are mainly produced using a variety of agricultural coproducts, such as hemp fiber and wheat straw; wood-based myco-composites are less frequent.[11] This is probably due to the much higher lignin content and the natural recalcitrance of wood, which makes fungal growth slower, producing less efficient materials.

In this context, reducing the recalcitrance of woody biomass through pretreatment could significantly increase the range of biomass available for myco-composite production. By breaking down structural barriers, pretreatments improve fungal colonization, increase porosity, and modify the fiber surface composition, making the biomass more accessible to mycelial growth.[12] These structural changes not only facilitate fungal colonization but also enhance the mechanical performance of biocomposites by strengthening the bond between the mycelium and the lignocellulosic matrix, ultimately leading to more durable and efficient materials.

However, for fungal growth to be effective, the pretreated substrate must have several key characteristics that are very different from those required for yeast or bacterial fermentation.[13] These characteristics can be categorized into several key factors: (i) Moisture content: fungi require a specific relative humidity level to thrive, typically around 80%. The substrate must retain enough water to support fungal growth without becoming overwatered. Excessive moisture could inhibit oxygen flow and lead to contamination. (ii) Air circulation: good air circulation within the substrate is crucial for fungal respiration. The substrate should be porous enough to allow oxygen to reach the growing mycelium while also enabling the release of carbon dioxide. (iii) Structural integrity: the substrate must maintain its structure to support the physical growth of the mycelium. It should not be too compact or too loose, ensuring that the mycelium can effectively bind the material together. (iv) Nutrient availability: the substrate and the growth medium should contain essential nutrients such as sugars and other organic nutrients, nitrogen, and minerals.

This study aims to optimize steam explosion pretreatments to enhance myco-composite production from beech wood using *Trametes versicolor*. Expanding on earlier findings that demonstrated the promising potential of steam explosion for stimulating fungal growth and colonization of beech wood by *T. versicolor*,[14] an in-depth analysis of this pretreatment was conducted. While this study focuses on beech wood, the ultimate objective is to apply these findings to post-consumer wood materials containing binders, namely, particle board and medium-density fiberboard (MDF). Steam explosion has shown potential for removing urea-formaldehyde adhesive from MDF,[15] which could allow this waste wood to be repurposed as a substrate for fungal growth. By first optimizing the process with beech wood, this study lays the groundwork for future applications in which post-consumer wood-treated MDF waste could serve as a biomass substrate for fungi in the development of myco-composites. Four experimental conditions were investigated to evaluate the impact of the treatment on wood characteristics that may influence myco-composite quality. The particle morphology, surface composition, and hydration behavior using techniques such as scanning electron microscopy (SEM), near-infrared spectroscopy (NIRS), Camsizer image analysis, goniometry, and water retention capacity were evaluated. Additionally, the liquid effluents from the process were analyzed by ion chromatography to provide a comprehensive understanding of the modifications induced by the pretreatment.

MATERIALS AND METHODS

Biological Materials. European beech (*Fagus sylvatica*) wood sourced from the Vosges region (France) was used as biomass (or substrate). The wood was initially reduced into small pieces before being ground into particles using a cross beater mill equipped with 8 mm sieves (Cross Beater Mill SK100, Retsch, Germany). Prior to inoculation with the fungus, the beech wood biomass was adjusted to a water content of 60%.

Steam Explosion Pretreatment. The steam explosion system (ADF, France) for material pretreatment involves a hydrothermal treatment. The wood particles, which had a moisture content of 6%, were initially vacuum-impregnated at 1 bar in a 1 L reactor with excess water for 20 min. This process ensured complete submersion of the particles. The relative water content after impregnation was as follows: 198% for beech, 235% for $R_{0\ 3.36}$, 248% for $R_{0\ 3.65}$, 378% for $R_{0\ 3.94}$, and 393% for $R_{0\ 4.24}$. Afterward, the liquid was removed, and 100 g of the wood particles were placed inside the SE reactor. High-temperature steam ranging from 180 to 210 °C was injected into the SE reactor for 5 or 10 min. The conditions used and corresponding sample nomenclature are given in Table 1. The calculated severity factors were calculated according to the equation defined by Overend and Chornet.[16] After the designated time, a pneumatic valve was opened, resulting in the bursting of biomass within the splitter due to the pressure difference. A mixture of liquid and solid components was recovered. The separation of effluents and exploded particles occurred in several steps: initially, a sieve was used to separate most of the particles. Afterward, centrifugation (Multifuge X4R Pro, Thermo Scientific, USA) and Buchner vacuum filtration with a 25 μm filter were combined. The exploded particles were then oven-dried at 103 °C for 24 h and stored under ambient conditions.

Table 1. Summary of Steam Explosion Conditions for Biomass Production

temperature (°C)	residence time (min)	pressure (MPa)	severity factor (R_0)	notation
180	10	1.6	3.36	$R_{0\ 3.36}$
190	10	1.9	3.65	$R_{0\ 3.65}$
210	5	2.8	3.94	$R_{0\ 3.94}$
210	10	2.8	4.24	$R_{0\ 4.24}$

https://doi.org/10.1021/acssuschemeng.5c00929
ACS Sustainable Chem. Eng. XXXX, XXX, XXX−XXX

Medium Preparation and Fungal Culture. All media were sterilized at 121 °C for 20 min before inoculation (vapor line 135-M, VWR, Germany). To establish the fungal culture, an initial growth of *T. versicolor* CTB 863 A was achieved on malt-agar medium containing 20 $g{\cdot}L^{-1}$ of malt extract and 2% agar for 7 days. Subsequently, five agar plugs (8 mm in diameter) were extracted from the *T. versicolor* cultures and inoculated into 250 mL baffled Erlenmeyer flasks containing 50 mL of malt medium (20 $g{\cdot}L^{-1}$).

These inoculated Erlenmeyer flasks were then incubated in an incubation shaker (Innova 44, New Brunswick Scientific, Germany) at 28 °C and 100 rpm for 2 days. Following this initial incubation, the culture was used to inoculate a sterile 2 L bioreactor filled with 1.5 L of malt medium (20 $g{\cdot}L^{-1}$) (Global Process Concept, PRO-LAB, France). The culture conditions were maintained at 28 °C, 80% O_2, 250 rpm, and pH 5. Probes were employed to monitor growth parameters, including temperature and oxygen levels, as well as redox potential and optical density (Figure S1). The redox potential was used as an indicator of the culture's health. A correlation between optical density and dry weight was used to monitor the growth of *T. versicolor* (Figure S2).

Once optimal growth conditions were achieved, the bioreactor content was harvested under sterile conditions. The mixture of medium and fungus was separated through centrifugation at 4200 rpm for 10 min at 21 °C (Multifuge X4R Pro, Thermo Scientific, USA). The supernatant was removed, while the fungus was used to produce the myco-composite.

Myco-Composite Production. The substrates were sterilized at 121 °C for 20 min. In a sterile Falcon tube, a ratio of 1:2 (W/V) of fungal mycelium was mixed with the sterilized substrate, with a 60% relative humidity achieved through effluent-mediated moisture adjustment. The falcon tubes were hermetically sealed with parafilm to allow air but not moisture to pass through. The culture falcon was then incubated (Binder KBF 240 climate chamber, Germany) at 28 °C for 14 days. Then, the myco-composites were unmolded and dried in an oven at 60 °C until they reached equilibrium moisture content, i.e., 6%. The production process is illustrated in Figure 1.

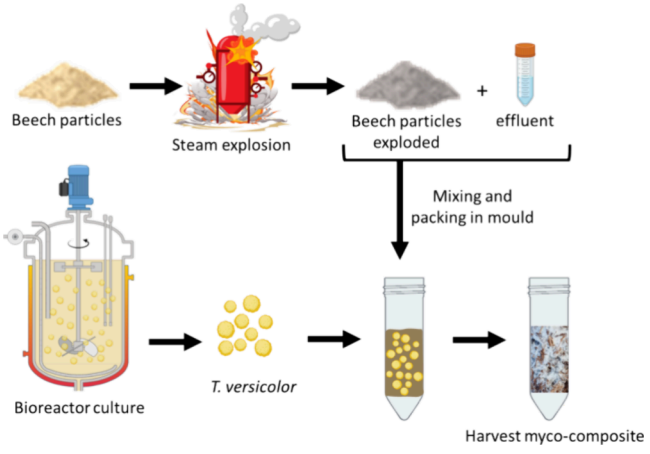

Figure 1. Illustration of the myco-composite production method.

Particle Size and Shape Analysis. A CAMSIZER P4 instrument (Retsch/Microtrac, Germany) was used to characterize the size and shape of wood particles before and after steam explosion. The device employs dynamic image analysis according to ISO 13322-2, with a measurement range of 0.02 to 30 mm. Dry particle samples (20 g) were analyzed using a dual-camera system and stroboscopic LED lighting. The system measured three key parameters: (i) xc_min: particle width (narrowest chord diameter); (ii) xFe_max: particle length (maximum distance between parallel tangents); and (iii) xMa_min: minimum width (smallest Martin diameter). A constant airflow (10 L/min) was used to improve fine particle analysis. The software ignored particles larger than 16 mm during the measurement process.

SEM. The SEM JEOL IT200 was used to analyze samples. Samples were coated with a Gold/Palladium 4.8 Å metallizer (ACE600 metallizer, LEICA, Germany). Samples were analyzed in high-vacuum mode with an SE detector. The working distance was 10 mm. The acceleration voltage and the probe current were set to 15 kV and 60%, respectively. The images were processed with ImageJ 1.54 d. To measure hyphal width, 10 hyphae were analyzed from 10 different images for each condition (n = 100).

Surface Hydrophobicity. Surface hydrophobicity was analyzed by using contact angle measurements. Wood disks were prepared by pressing the material at 20 tons with a manual press (Vaneox 25t manual, FluXana, Germany) to create a flat surface. A drop shape analyzer (DSA) (FM40 EasyDrop, Krüss, Germany) with associated software was used for measurements. The contact angle was determined by placing a water drop on the wood surface (1.95 mm diameter drop). Due to rapid absorption, analysis focused on the first 2 s after drop placement. Each sample was tested at least three times to ensure accuracy.

Infrared Spectroscopy. To provide quick identification of the main components in myco-composites, mid-infrared (MIR) and near-infrared (NIR) analyses were used. They were performed on native and steam explosion pretreated beech particles, as well as ground myco-composite samples. An infrared spectrometer (Spectrum 100 IR/NIR, PerkinElmer, USA) with an InGaAs detector and a CaF2 beam splitter was used for the analysis. Spectra were collected from 10,000 to 4000 cm^{-1} with 2 cm^{-1} resolution. For each sample, 20 spectra were averaged. Data processing was carried out using RStudio (Version 2023.12.1 + 402) with the ChemoSpec plugin.[17] Second derivatives were calculated from the raw NIR spectra.[18] Principal component analysis (PCA) was performed on the entire spectrum to cluster samples based on their physicochemical properties. The PCA scores and loadings were then analyzed to identify the most influential variables for each principal component.[15]

Water-Binding Capacity of Wood and Pretreated Wood. The impact of steam explosion on the sorption properties of the wood was quantified. 30 g of particles were placed in a container to which 150 mL of distilled water was added. The entire mixture was then autoclaved at 121 °C for 20 min. Following autoclaving, the contents of the container, including the particles and excess liquid, were filtered. The excess liquid was subsequently transferred to a graduated tube to measure the volume of water remaining in the container that had not been absorbed by the material.

Water Effluent Sugar Quantification. The sugars present in the effluents from the SE process were analyzed by using high-performance anion exchange chromatography coupled with pulsed amperometric detection (HPAEC-PAD) (Dionex ICS-3000). The separation was performed on a CarboPac PA20 column (Dionex) using a gradient of water, sodium hydroxide (NaOH), and sodium acetate ($C_2H_3NaO_2$) as eluents. External standards of sugars and uronic acids were used for calibration (all provided by Sigma-Aldrich).

Quantification of HMF and Furfural in Water Effluents. The HMF and furfural were quantified using high-performance liquid chromatography coupled with a diode array detector (HPLC-DAD) (Dionex UltiMate 3000 DAD). The separation was performed on an XBridge Shield RP18 column, using water and acetonitrile as eluents. Standards of furfural and HMF were used to establish the calibration curve, with detection at 300 nm.

Compressive Strength of Myco-Composites. Compressive strength was evaluated following the ASTM C165-17 standard (ASTM, 2017). Cylindrical samples with dimensions of 30 mm in diameter and 40 mm in length were used for testing. Each specimen was subjected to compression of up to 40% deformation at a constant rate of 1 mm/min using a universal mechanical testing machine (Xforce P, Zwick Roell, Germany).

For shape recovery analysis, after compressing the samples to 40%, the load was released, and thickness recovery was measured immediately and again after 5 min. Thickness recovery after 5 min was calculated using eq 1:

https://doi.org/10.1021/acssuschemeng.5c00929
ACS Sustainable Chem. Eng. XXXX, XXX, XXX−XXX

Figure 2. Macroscopic modification of wood particles caused by steam explosion. Severity coefficient are as follows: *A* = native, *B* = $R_{0\ 3.36}$, *C* = $R_{0\ 3.65}$, *D* = $R_{0\ 3.94}$, and *E* = $R_{0\ 4.24}$. The scale bar is 1 cm.

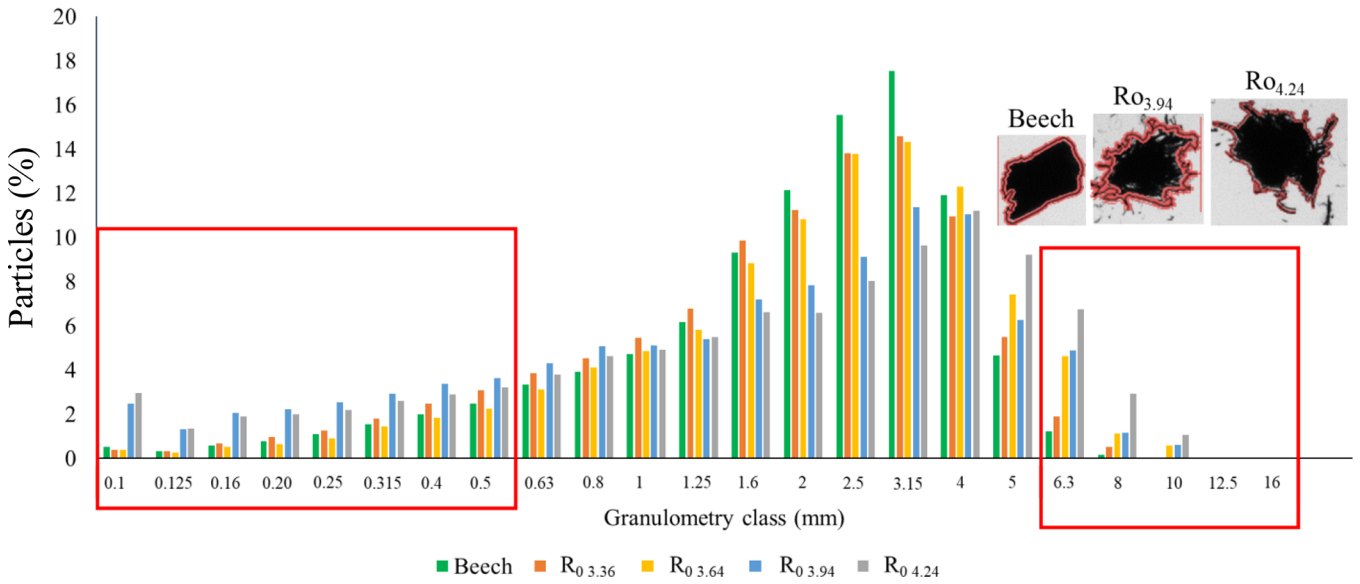

Figure 3. Narrowest particle width distribution (xMa_min).

$$\text{thickness recovery}(\%) = \frac{(e_{5\text{min}} - e_{\text{aftercompression}})}{(e_{\text{initial}} - e_{\text{aftercompression}})} \times 100 \quad (1)$$

where e_{initial} is the initial thickness, $e_{\text{after compression}}$ is the thickness measured immediately after compression, and $e_{5\ \text{min}}$ is the thickness measured after 5 min.

RESULTS AND DISCUSSION

1. Particle Characterization. *1.1. Morphological Analysis.* Beech wood particles were treated by SE according to four combinations of residence time and temperature (Table 1). The calculated severity factors are also given and will be used thereafter as the sample name. As expected, the more severe the treatment, the more the particles were defibrated and showed a fluffy appearance (Figure 2). As the severity factor increased, the particles changed color from creamy white to dark brown. The visual inspection of the biomass suggested that mild SE conditions ($R_{0\ 3.36}$ and $R_{0\ 3.65}$) did not strongly alter the particle morphology. The differences between native beech particles and those with a R_0 of 3.36 were barely noticeable. On the contrary, the $R_{0\ 4.24}$ particle sample mostly consisted of a fluffy mixture of single fibers or small fiber bundles. As the severity of wood pretreatment increased, the degree of defibration enhancement became more pronounced.[19]

Automated imaging techniques were used to quantitatively assess how SE impacts the macrostructure of wood through particle morphology characterization. The data obtained after particle size and shape analysis (CAMSIZER analysis) are shown in Figure 3. Despite all the samples being characterized by a maximum modal particle size value of 3.15 mm, the samples can be subdivided into two clusters. The cumulative fraction of fine particles (<500 μm) was found to be significantly (ANOVA, $P < 0.05$) more abundant for $R_{0\ 3.94}$ and $R_{0\ 4.24}$ (4.6 ± 0.9 and 11.6 ± 3.3%, respectively) than for $R_{0\ 3.36}$ and $R_{0\ 3.65}$ or native beech (around 0.7%). $R_{0\ 4.24}$ was also the most frequent in the particles of size above 5 mm. Additionally, the total number of counted particles was similar for $R_{0\ 3.36}$ and $R_{0\ 3.65}$ or native beech (535,231 ± 57,360) but 11 times lower than that in $R_{0\ 3.94}$ (5,921 811 ± 952,488) and about 27 times lower than that in $R_{0\ 4.24}$ (14,310,749 ± 705,795). Further examination of the particle shape (Figure 3) showed that particles <500 μm were isolated fibers, whereas those above 5 mm were fiber aggregates. This agglomeration is due to electrostatic forces during measurement.[20] The quantitative analysis of width and length particle morphology for fine and aggregate distributions is given in Figure S3. Analysis of data collected from a large sample of particles revealed a correlation between the severity factor and the extent of wood modification. Specifically, higher severity factors ($R_{0=3.94}$ and $R_{0=4.24}$) were associated with significant wood defibration. In contrast, lower-severity factors ($R_{0\ 3.36}$ and $R_{0\ 3.65}$) primarily affected the wood's ultrastructure without causing extensive defibration. This distinction suggests that the severity of SE treatment directly influences the degree and nature of changes in the wood structure.

To get a comprehensive understanding of the SE conditions on wood microstructures, beech wood particles were inves-

https://doi.org/10.1021/acssuschemeng.5c00929
ACS Sustainable Chem. Eng. XXXX, XXX, XXX−XXX

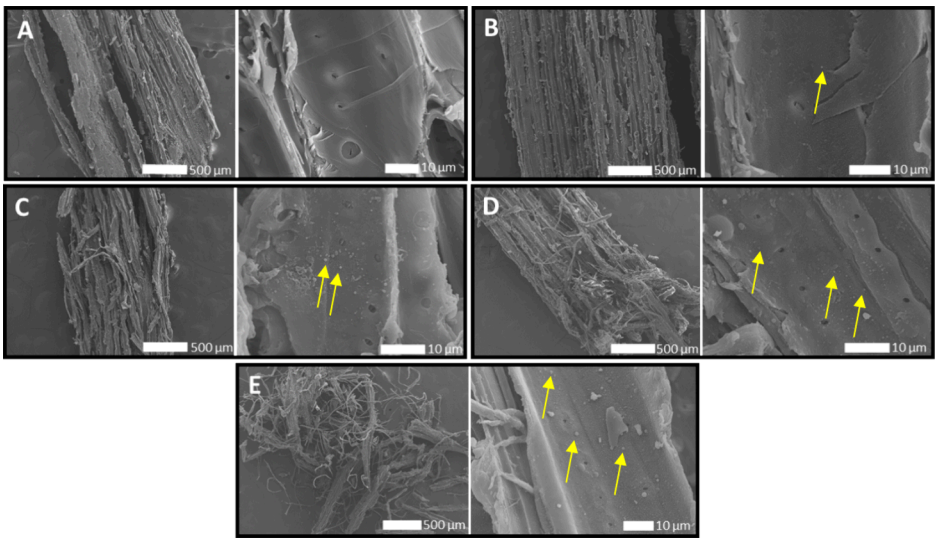

Figure 4. Scanning electron microscopy (SEM) observation of wood particles before and after a steam explosion. Low-magnification SEM image (left) and high-magnification SEM image (right). (A) Beech, (B) $R_{0\ 3.36}$, (C) $R_{0\ 3.65}$, (D) $R_{0\ 3.94}$, and (E) $R_{0\ 4.24}$. Yellow arrows: lignin deposit.

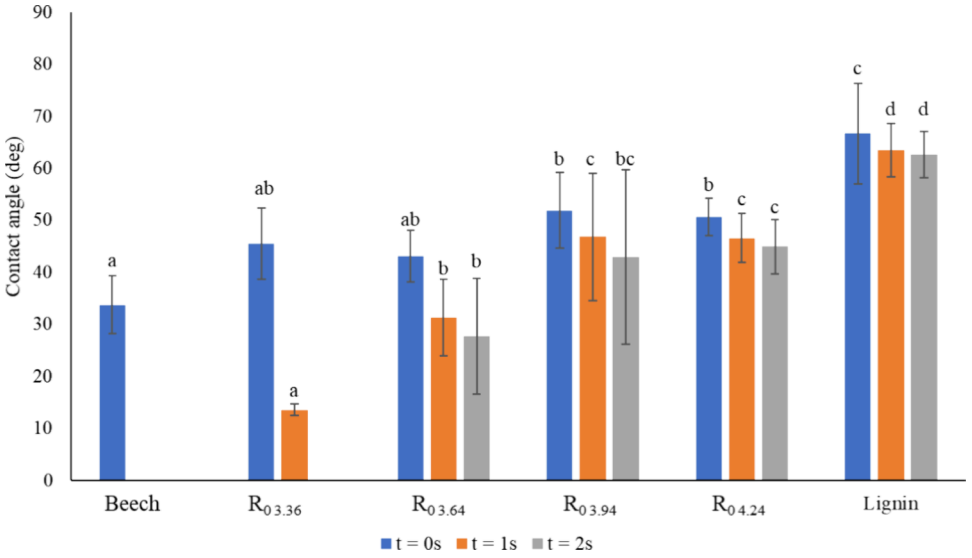

Figure 5. Surface hydrophobicity modification of particles by steam explosion analyzed by a drop shape analyzer. Letters indicate groups that are significantly different (ANOVA, $p < 0.05$, post hoc Tukey HSD analysis).

tigated by SEM. Low-magnification observations confirmed a correlation between the increase in the severity factor and the intensity of wood defibration (Figure 4). On native beech wood particles, the wood cell structure was observed, with vessels and fibers tightly packed together. On samples treated with mild conditions, $R_{0\ 3.36}$ and $R_{0\ 3.65}$ showed a noticeable change in the surface of the beech particles. At high severities, the surface became blistered, and burrs were clearly visible, confirming the wood particle defibration observed earlier. The entire cell wall was modified as the severity of the SE treatment increased.

1.2. Surface Properties. The surface hydrophobicity of wood particles directly impacts the ability of fungi to colonize and form strong mycelial networks, which are crucial for myco-composite production.[12] While hydrophobic surfaces may limit initial attachment and growth, hydrophilic surfaces can provide better water and nutrient retention but must be balanced to avoid excessive moisture.[21] The literature widely reports that steam explosions can lead to the deposition of lignin droplets on the surfaces of cell walls,[22,23] potentially affecting their hydrophobicity. To evaluate the effects of steam explosion (SE) on the hydrophobicity of wood particles, disk-shaped samples were prepared by pressing the particles under a pressure of 20 tons. This approach ensured a uniform and flat surface for each sample, which was essential, as reliable contact angle measurements could not be obtained from irregular, isolated particles. While such high-pressure processing could theoretically influence surface properties, this potential bias was addressed through a complementary surface roughness analysis (Figure S4).

The roughness analysis revealed that native beech pellets exhibited a significantly higher surface roughness (Ra = 189 μm) compared to steam-exploded beech samples, which showed an average Ra of 68 μm (Figure S5). This supports the hypothesis that SE, through increased defibration, leads to smoother surfaces. As a result, variations in hydrophobicity measurements can be more confidently attributed to chemical and structural changes induced by the SE treatment rather than differences in surface topography. Moreover, the relatively consistent rough-

https://doi.org/10.1021/acssuschemeng.5c00929
ACS Sustainable Chem. Eng. XXXX, XXX, XXX−XXX

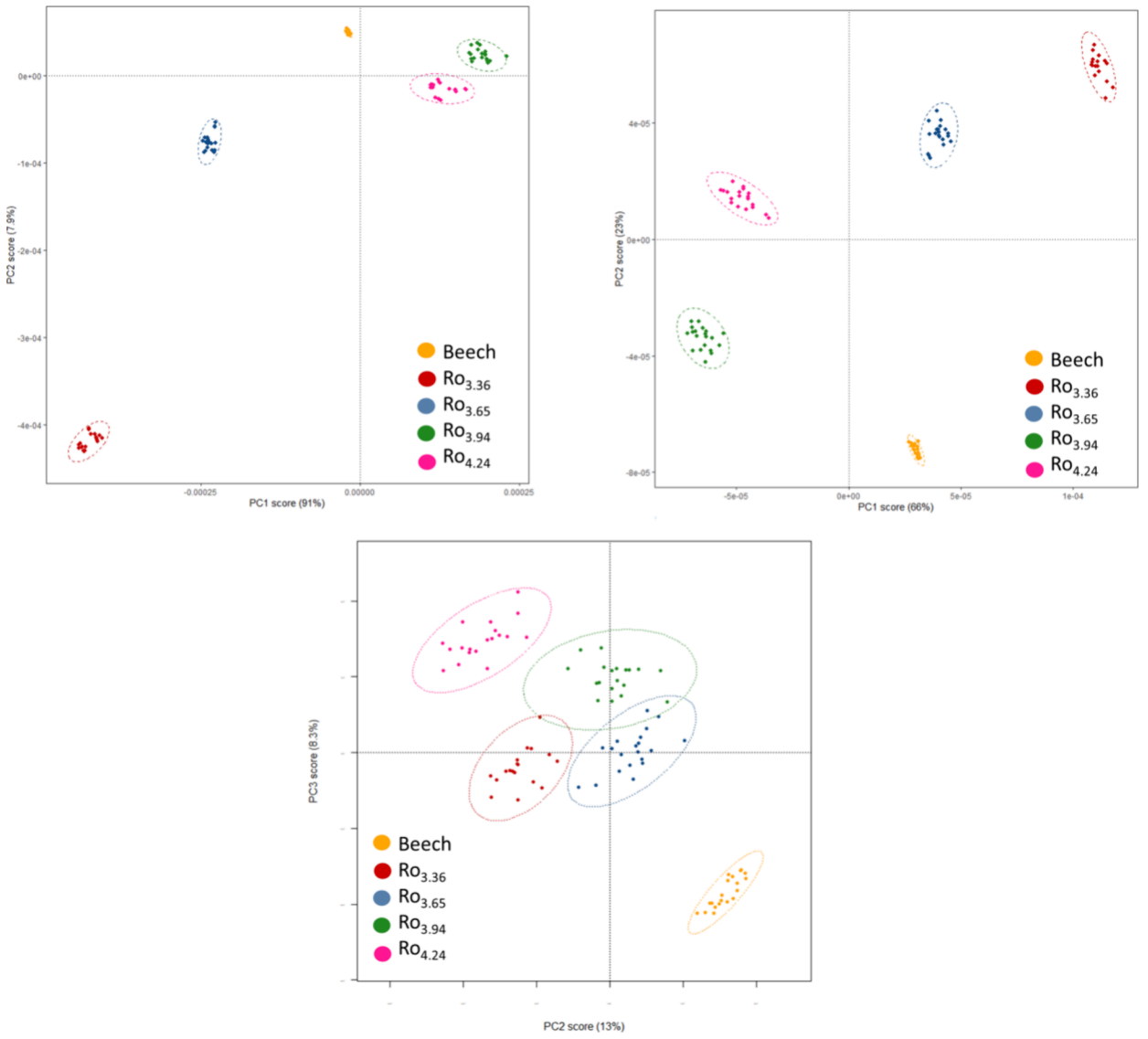

Figure 6. PCA on the subregion of interest. (A) PCA from 5450 to 5100 cm^{-1} with PC1 and PC2. (B) PCA from 4955 to 4600 cm^{-1} with PC1 and PC2. (C) PCA from 6000 to 5750 cm^{-1} with PC2 and PC3. Clear discrimination between native beech particle, low severity factor ($R_{0\ 3.36}$ and $R_{0\ 3.65}$), and high-severity factor ($R_{0\ 3.94}$ and $R_{0\ 4.24}$).

ness observed across SE-treated samples allows for a valid and meaningful comparison of their hydrophobic behavior. This highlights the intrinsic link between the hydrophobicity and the fundamental characteristics of the substrate.

The hydrophobicity of native SE-treated beech wood particles and lignin pellets was measured using a DSA. The increase in contact angle reflects an increase in the material's surface hydrophobicity. As wood is a very hygroscopic material, contact angle measurements were performed at t = 0, 1, and 2 s. The results are plotted in Figure 5. For native beech, an initial contact angle of 33.7° (±5.6°) was observed, with complete drop absorption occurring within 1 s. As SE treatment severity increased, both the initial contact angle and the persistence of the droplet on the surface increased: at $R_{0\ 3.36}$, only 73% of the droplet was absorbed after 1 s; at $R_{0\ 3.65}$, absorption dropped to 28%. Under the most severe SE conditions ($R_{0\ 3.94}$ and $R_{0\ 4.24}$), as well as for pure lignin, only around 5% of the droplet was absorbed after 2 s. These observations illustrate the increase in the overall surface hydrophobicity of the particles according to the increase in treatment severity. For $R_{0\ 4.24}$, the hydrophobicity tends toward that of pure lignin, with initial angles of 50.6° (±3.6°) and 45° (±5.2°) after 2 s.

1.3. Chemical Composition. The surface modifications of the beech particles were also examined by NIRS. This non-destructive method was successfully used to monitor the effect of the SE on the wood biomass.[15,22,24] After spectral acquisition and the calculation of the secondary derivative, three zones with high variability between the samples were identified on the spectra. The first region was located between 6000 and 5750 cm^{-1}, the second between 5450 and 5100 cm^{-1}, and the third was located from 4955 to 4600 cm^{-1} (Figure S6). PCA was used in order to develop a clustering analysis of the samples subsequent to NIRS. PCA is a statistical technique used to reduce the dimensionality of data and to explore relationships between variables. This analysis was performed on each of the three regions of variability on the second derivative, and the associated loading analysis was performed (Figure 6). The loading analysis allowed the identification of the variables that made the highest contribution to the intersample variability on each of the principal components. Independently of the spectral

https://doi.org/10.1021/acssuschemeng.5c00929
ACS Sustainable Chem. Eng. XXXX, XXX, XXX−XXX

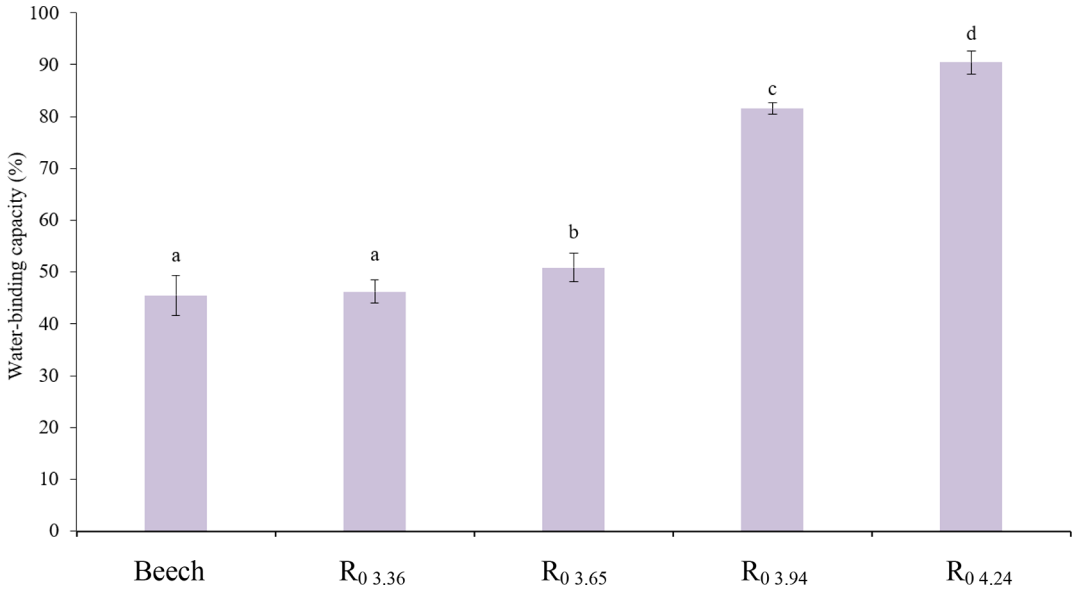

Figure 7. Water-binding capacity of wood and pretreated wood. Letters indicate groups that are significantly different (ANOVA, $p < 0.05$, post hoc Tukey HSD analysis).

Table 2. Composition of the SE Water Effluent in Monosaccharides and Furan Derivatives as a Function of SE Severity[a]

	$R_{0\ 3.36}$		$R_{0\ 3.65}$		$R_{0\ 3.94}$		$R_{0\ 4.24}$	
component	before PH	after PH	before PH	after PH	before PH	after PH	before PH	after PH
Fuc[b]	13.7 ± 0.4	11.6 ± 1.3	7.9 ± 1.3	8.2 ± 15.0	6.1 ± 0.5	5.5 ± 0.3	6.2 ± 0.4	5.6 ± 0.3
Rha[c]+Ara[d]	241.4 ± 16.4	534.7 ± 62.3	183.5 ± 38.6	441.6 ± 55.4	163.9 ± 1.2	253.6 ± 7.6	190.6 ± 4.1	237.7 ± 15.9
Gal[e]	35.2 ± 2.0	226.6 ± 18.1	49.3 ± 9.7	287.5 ± 35.9	45.2 ± 0.2	148.5 ± 8.6	56.9 ± 1.4	151.8 ± 17.9
Glc[f]	40.4 ± 3.2	444.2 ± 43.6	103.3 ± 19.2	304.0 ± 37.4	40.3 ± 0.8	277.3 ± 9.3	61.1 ± 2.0	312.4 ± 16.3
Xyl[g]	176.3 ± 10.0	4933.9 ± 523.3	199.6 ± 40.5	4289.0 ± 507.3	663.3 ± 4.4	4825.5 ± 167.6	952.0 ± 10.4	4666.0 ± 311.0
Man[h]	8.6 ± 1.1	507.8 ± 69.0	8.7 ± 2.4	265.2 ± 41.5	34.4 ± 1.2	462.9 ± 34.6	64.3 ± 3.8	559.1 ± 110.3
GalUA[i]	0.0	437.7 ± 59.7	0.0	396.3 ± 52.4	0.0	174.4 ± 11.5	0.0	125.7 ± 8.2
Ac glucu.[j]	0.0	23.0 ± 3.7	0.0	23.6 ± 1.6	0.0	10.0 ± 1.6	0.0	8.8 ± 0.3
furfural	16.8 ± 0.9		92.4 ± 1.9		151.3 ± 8.3		334.3 ± 1.1	
HMF[k]	3.1 ± 0.1		10.0 ± 2.6		15.8 ± 0.4		38.3 ± 0.1	

[a]All data are given in mg·L^{-1} [b]Fucose. [c]Rhamnose. [d]Arabinose. [e]Galactose. [f]Glucose. [g]Xylose. [h]Mannose. [i]Galacturonic acid. [j]Glucuronic acid. [k]Hydroxymethylfurfural.

region considered for the PCA, the samples were successfully clustered according to the severity of the SE treatment. It was possible to delineate three groups: the group containing only native beech, a second group with $R_{0\ 3.36}$ and $R_{0\ 3.65}$, and a third group with $R_{0\ 3.94}$ and $R_{0\ 4.24}$. In detail, PCA of the range 5450 to 5100 cm^{-1} showed water fixation on PC1 (Figure 6A). PC2 was associated with an alteration of the cellulose crystallinity and the degree of polymerization (DP). This is consistent with previous findings.[25] The PCA in the range from 4955 to 4600 cm^{-1} showed similar results (Figure 6B). Based on band assignment and loading analysis, the PCA of the range from 6000 to 5750 cm^{-1} was more relevant to characterize the SE effect on the wood cell wall (Figure 6C). Indeed, variability on the PC2 axis was attributed to the hemicellulose content and lignin to PC3. The sample clustering clearly exhibited a linear relation between the severity of the condition and the lignin to hemicellulose ratio. NIRS analysis on the wood particles suggested that the more severe the treatment, the more the lignin was relocated to the cell wall surface, which is confirmed by MIR analysis (Figure S7). Additionally, the increase in the SE treatment severity triggered strong hemicellulose removal and possibly an *in situ* chemical modification. Taken together, NIRS and MIRS analyses provided chemical complementary data to the SEM observations.

1.4. Water Retention Capacity. The water-binding capacity of both untreated and pretreated wood was assessed to optimize fungal growth, as the moisture content significantly influences fungal development in the material.[21] Compared to native wood, particles pretreated at $R_{0\ 3.36}$ and $R_{0\ 3.65}$ showed no significant change in water-binding capacity (around 45%), while a significant increase, between 80 and 90%, was observed at the highest severities ($R_{0\ 3.94}$ and $R_{0\ 4.24}$) (Figure 7). This can be explained by the effects of pretreatment discussed above: the wood fiber separation, the strong alterations in carbohydrate distribution, and the hydrolysis and relocation of lignin, which improve polysaccharide accessibility. As a result, the wood particles treated at $R_{0\ 3.94}$ and $R_{0\ 4.24}$ display a high surface exchange and, in turn, bind more water than native wood.

2. SE Liquid Phase Analysis. It is well known that the uncatalyzed SE process has a strong impact on noncellulosic wood polysaccharides, which are partially hydrolyzed by autohydrolysis mechanisms and recovered in the liquid phase of the process.[26] Depending on the reaction conditions, pentose and hexose dehydration reactions can also take place to form furan derivatives. The concentrations of the main beech

https://doi.org/10.1021/acssuschemeng.5c00929
ACS Sustainable Chem. Eng. XXXX, XXX, XXX−XXX

monosaccharides contained in the aqueous phases were quantified for the four pretreatment severities. Quantification by ion chromatography was carried out before and after a controlled hydrolysis step to determine the total concentrations of simple sugars and oligosaccharides in the effluents. Effluent contents of furfural and hydroxymethylfurfural (HMF) are also given in Table 2.

Sugars of the main hemicelluloses of beech wood were detected mainly in the form of polysaccharides. It is observed that, in agreement with previous work, increasing the severity of the SE treatment leads to an increase in monosaccharide concentration in the effluent.[26] As expected, xylose, originating from wood xylans, is the dominant sugar, with concentrations of around 5 $g{\cdot}L^{-1}$. Furfural and HMF, produced by dehydration reactions of pentoses (primarily xylose) and hexoses, respectively, were also detected. In line with the literature, a significant increase in concentration is observed with increasing severity of the SE treatment. Furfural and HMF are toxic molecules well known for inhibiting the metabolism of microorganisms. The work of Nilsson et al.[27] tested the growth of *T. versicolor* in the presence of HMF and furfural at concentrations of 0.2 and 0.6 $g{\cdot}L^{-1}$, respectively. Their results showed that at these concentrations, these molecules did not significantly inhibit the growth of *T. versicolor*. A slight reduction in growth was observed after 2 days in the presence of the inhibitors, but after 5 days, growth was equivalent with or without the inhibitors. Furthermore, it was previously shown that furfural and HMF can be metabolized by *T. versicolor*.[27] In the present work, the maximum concentrations measured of furfural and HMF (corresponding to the highest severity condition $R_{0\ 4.24}$) were 0.33 and 0.04 $g{\cdot}L^{-1}$, respectively. These values are significantly lower than those studied by Nilsson et al.[27] for which no inhibitory effect was observed. Based on these preliminary works, we can conclude that the inhibitors contained in the SE effluent are not in sufficient concentrations to explain the fungal growth inhibition. It can therefore be concluded from this study that the aqueous effluents produced by SE, rich in complex sugars and containing low concentrations of potentially inhibitory substances, can constitute a nutrient medium for the growth of *T. versicolor*.

3. Myco-Composite Production. Materials and Methods (Figure 9) Native and pretreated beech wood particles in combination with their respective aqueous effluents were used to produce myco-composites, as described in Figure 1. NIRS was used successfully to quantify the fungal colonization in myco-composites.[14] More precisely, principal component 2 (PC2) was correlated with nitrogen content originating from fungal cell wall content (protein and chitin). Building on this approach, we utilized PC2 to investigate the relationship between fungal colonization and substrate bulk density. Our findings revealed that colonization was more pronounced in substrates treated at $R_{0\ 3.36}$, $R_{0\ 3.65}$, and $R_{0\ 3.94}$, while native beech and $R_{0\ 4.24}$ exhibited significantly lower colonization levels (Figure 8). The substrate bulk density provides an integrated value resulting from changes in the chemical composition, cellulose accessibility, lignin relocation, and fiber separation. These results underscore the critical influence of substrate bulk density on fungal colonization, with both particle density and fiber morphology playing crucial roles in fungal growth dynamics.

Based on these observations, we categorized the substrates into two distinct groups: (i) untreated beech wood and beech wood treated at $R_{0\ 4.24}$ and (ii) substrates subjected to lower-

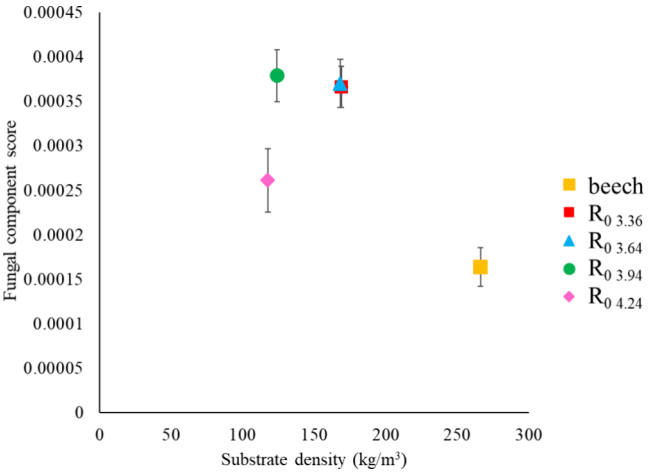

Figure 8. Fungal component score as a function of substrate density.

severity treatments at $R_{0\ 3.36}$, $R_{0\ 3.65}$, and $R_{0\ 3.94}$. Within-group comparisons are valid, as biomass treatment remains the primary variable. However, cross-group comparisons are not feasible due to differing colonization patterns between the two groups.

Macroscopic observations of samples A, B, and C confirm that colonization with $R_{0\ 3.36}$, $R_{0\ 3.65}$, and $R_{0\ 3.94}$ is more effective than with beech particles, and $R_{0\ 4.24}$ particles, reaching an optimum at $R_{0\ 3.65}$, validating our previous study[11] (Figure 9). This trend,

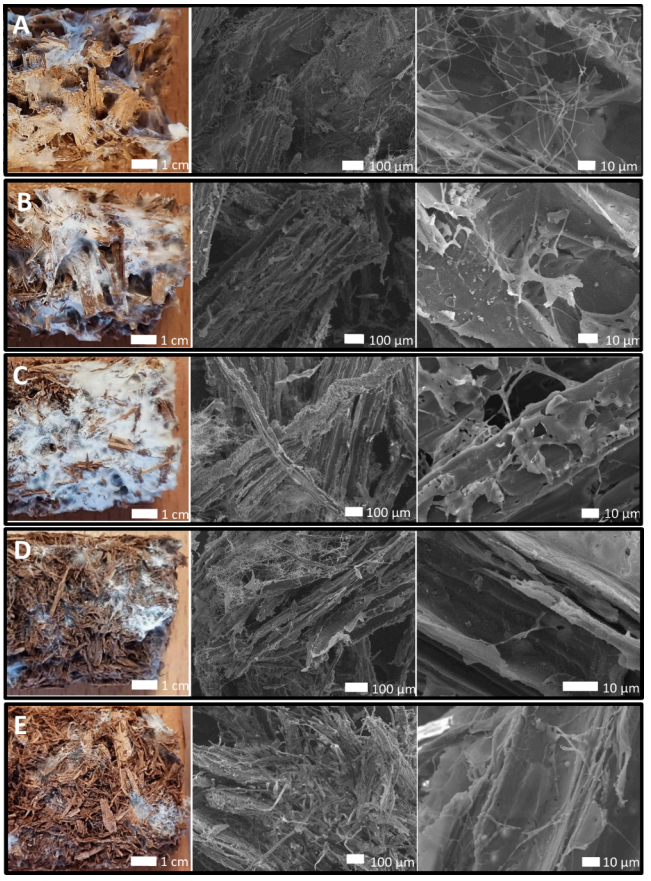

Figure 9. Macroscopic pictures after 14 days of growth (white: fungus and dark brown: wood particles) and scanning electron microscopy (SEM) observations of the myco-composite. (A) Beech, (B) $R_{0\ 3.36}$, (C) $R_{0\ 3.65}$, (D) $R_{0\ 3.96}$, and (E) $R_{0\ 4.24}$.

https://doi.org/10.1021/acssuschemeng.5c00929
ACS Sustainable Chem. Eng. XXXX, XXX, XXX−XXX

supported by SEM data, demonstrates an increase in hyphal density and diameter as a function of SE treatment severity. The average hyphal sizes for the most severe conditions ($R_{0\ 3.94}$ and $R_{0\ 4.24}$) are 0.4 ± 0.1 and 0.5 ± 0.1 μm, respectively. In contrast, less severe conditions ($R_{0\ 3.36}$ and $R_{0\ 3.65}$) result in hyphae that are approximately twice as thick, with diameters of 0.9 ± 0.1 and 1.3 ± 0.1 μm, respectively. Interestingly, myco-composites produced with native beech wood exhibit hyphae with diameters similar to those observed under severe treatment conditions (0.2 ± 0.1 μm). These observations are consistent with findings from our previous study by Aguilar et al.,[14] who reported similar trends in hyphal diameter variations in response to different severities of SE pretreatment on softwood substrates.

SEM observations also showed a higher density of extracellular polymeric substance (EPS) matrix for hyphae developing on $R_{0\ 3.36}$ and $R_{0\ 3.65}$ substrates. This EPS matrix is known to play a major role in fungal adhesion to the wood substrate by providing a transient junction between the hyphae and the wood, thus establishing a point of attachment to the site of degradation.[28,29] Extracellular enzymes and structural proteins were localized in the EPS.[30,31] The production of EPS was shown to be triggered upon the sensing of a suitable substrate.[32,33] The density of fungal colonization and hyphal morphology were correlated with the mechanical properties of the myco-composite materials.[34,35] In this study, we observed higher fungal colonization with thicker hyphae, higher EPS secretion, and trimitic morphology in the myco-composite produced with $R_{0\ 3.65}$. Taken together, our results suggest that fungal colonization and hyphal cohesion might change the mechanical performance of the myco-composite materials. Compression tests and thickness recovery were successfully used to evaluate the link between hyphal network density, hyphal binding to wood, and mechanical properties.[36−38] Interestingly, myco-composite material produced from poorly colonized substrates ($R_{0\ 4.24}$ and beech) showed similar Young's modulus values (9.10^{-4} MPa) to those measured from $R_{0\ 3.94}$ myco-composites (Figure 10a). This suggests that these

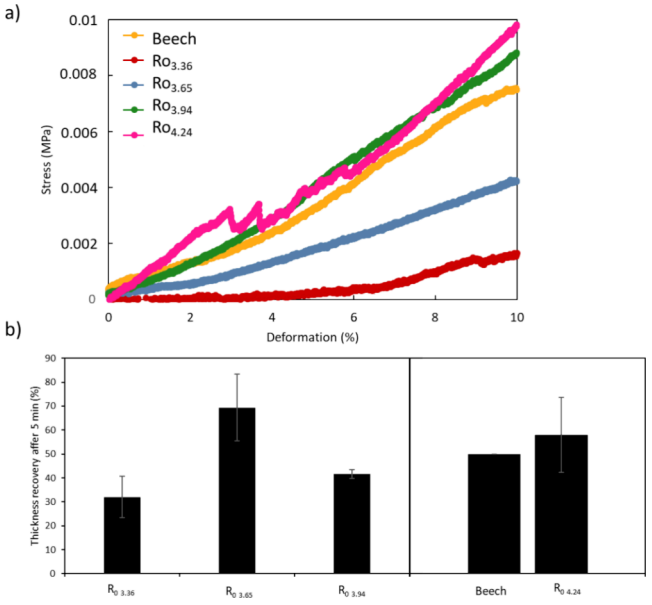

Figure 10. (a) Stress−strain curve of the myco-composite materials. (b) Thickness recovery of the myco-composites following a 5 min compression period (ANOVA, $p < 0.05$, post hoc Tukey HSD analysis).

composites have an internal structure and microporosity close to native wood. The compression test results obtained for fungal $R_{0\ 3.94}$ myco-composites did not differ from the $R_{0\ 4.24}$ and beech ones. Thus, despite fungal colonization being similar in $R_{0\ 4.24}$, beech, and $R_{0\ 3.94}$ myco-composites, we conclude that the network observed in $R_{0\ 3.94}$ myco-composites was only poorly cohesive. By comparison, myco-composites obtained with $R_{0\ 3.36}$ and $R_{0\ 3.65}$ substrates exhibited higher flexibility and a significantly lower Young's modulus (2.10^{-4} and 4.10^{-4} MPa, respectively). Thus, a very similar colonization level but with different amounts of EPS and hypha morphology leads to a contrasting stiffness behavior. To further investigate the possible influence of the mycelium properties on the myco-composite material, thickness recovery tests were performed. The results showed significant variation in the structural integrity of the myco-composites despite comparable fungal growth (Figure 10b). Myco-composites produced from $R_{0\ 3.65}$ achieved the highest thickness recovery (69 ± 14%) compared to myco-composites produced from $R_{0\ 3.36}$ and $R_{0\ 3.94}$ (respectively 32 ± 8 and 41 ± 2%), suggesting optimal substrate accessibility for fungal colonization and material cohesion. The complex and dense mycelial network within myco-composites produced from $R_{0\ 3.65}$ might restrict the movement of wood chip particles and result in better mechanical and cushioning properties.

To gain a deeper understanding of how the physical and chemical parameters of biomass resulting from the SE pretreatments influence myco-composite performance, we divided the main influencing factors into four categories, each represented in a separate graphical visualization: (a) macro-scale substrate characteristics, (b) substrate wood cell wall alterations, (c) myco-composite fungal colonization behavior, and (d) myco-composite mechanical properties (Figure 11).

Figure 11a illustrates the relationship between fiber defibration and bulk density. An inverse correlation is observed: as the degree of defibration increases, the bulk density of the substrate decreases significantly, from 266 kg/m^3 in untreated wood to 118 kg/m^3 at the highest SE severity. This reflects the increasing porosity and loosened structure of the biomass as hemicelluloses are solubilized and the fiber network is disrupted. These macrostructural changes are critical, as they directly affect the material's ability to retain moisture and support fungal growth.

The second graph focuses on chemical and surface modifications at the cellular level (Figure 11b). As expected, surface lignin content shows an inverse relationship with surface wettability: increased lignin deposition, particularly after high-severity SE, corresponds to higher hydrophobicity. Additionally, the progressive breakdown of polysaccharides and exposure of cellulose during SE treatment improves the water retention capacity. These trends suggest that moderate SE conditions (notably $R_{0\ 3.65}$) produce a substrate with optimal surface hydrophilicity and internal moisture regulation, two key factors supporting fungal adhesion and sustained growth.

Figure 11c highlights the variability in fungal colonization across different substrates. Notably, despite similar colonization patterns for $R_{0\ 3.36}$, $R_{0\ 3.65}$, and $R_{0\ 3.94}$, significant differences in hyphal morphology were apparent. The diameters of hyphae varied widely, with larger diameters associated with substrates treated under moderate SE conditions. This suggests that fungal physiology is responsive to substrate accessibility and nutrient availability, parameters that are optimized under intermediate SE severities, likely due to an ideal balance of chemical cues, porosity, and moisture content.

https://doi.org/10.1021/acssuschemeng.5c00929
ACS Sustainable Chem. Eng. XXXX, XXX, XXX−XXX

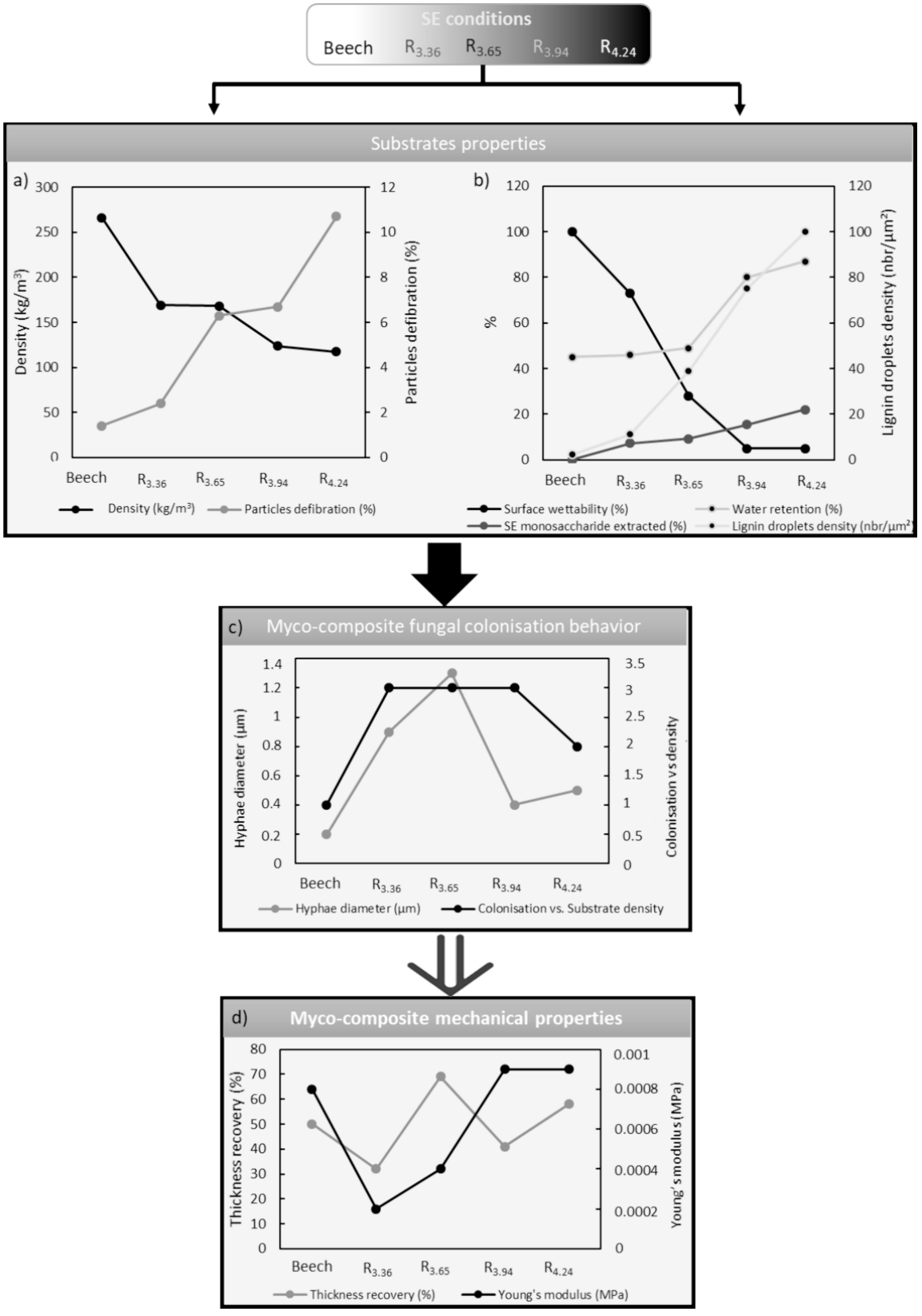

Figure 11. Analysis of the cascade of effects triggered by biomass SE pretreatment, from substrate modification to final myco-composite properties: (a) substrate macrostructural properties, (b) biomass wood cell wall alteration, (c) fungal colonization, and (d) mechanical properties of myco-composites.

The final graph examines the mechanical performance of myco-composites (Figure 11d). Substrates rich in wood fibers or with intact mycelial structures showed the highest thickness recovery after compression ($R_{0\ 3.65}$), reflecting strong structural

https://doi.org/10.1021/acssuschemeng.5c00929
ACS Sustainable Chem. Eng. XXXX, XXX, XXX−XXX

cohesion. In contrast, materials derived from over-defibrated or poorly colonized substrates ($R_{0\ 3.36}$ and $R_{0\ 4.24}$) showed insufficient mycelial density and low mechanical resilience. The myco-composite produced under $R_{0\ 3.65}$ conditions always showed the best mechanical properties, attributable to a well-balanced fiber network, optimal colonization, and sufficient moisture retention.

Together, these four visualizations provide a comprehensive framework for understanding how SE pretreatment affects the key physicochemical parameters that govern the performance of myco-composites. They demonstrate that optimal outcomes are not achieved under the most severe processing conditions, but rather through a moderate SE severity (e.g., $R_{0\ 3.65}$), where trade-offs between substrate structure, fungal behavior, and composite strength are best managed.

CONCLUSIONS

In conclusion, SE pretreatment significantly modifies the physical and chemical properties of beech wood particles, enhancing their suitability as substrates for myco-composite production. Increasing the severity factor (R_0) improves defibration, water retention, and surface hydrophobicity while releasing sugars with minimal accumulation of inhibitory compounds such as furfural and HMF. These modifications improve substrate bioavailability and support fungal colonization. Importantly, an intermediate SE severity yielded optimal results. Excessive severity ($R_0 > 3.7$) impaired fungal development due to adverse changes in wood-water interactions. This finding highlights the critical role of pretreatment severity in balancing substrate accessibility and nutrient preservation.

Although moderate SE pretreatment incurs additional energy input, the resulting improvements in fungal growth and composite performance justify this approach. These findings support SE as a tunable and sustainable strategy for converting lignocellulosic biomass into high-performance myco-composite materials. By initially optimizing the process with beech wood, this study sets the stage for future applications where post-consumer-treated MDF waste could be repurposed as a fungal biomass substrate for myco-composite fabrication, enabling scalable, cost-effective production with minimal environmental impact.

ASSOCIATED CONTENT

Supporting Information

The Supporting Information is available free of charge at https://pubs.acs.org/doi/10.1021/acssuschemeng.5c00929.

Surface roughness quantification materials and methods, growth monitoring of fungal pellets as a function of time, correlation between optical density and dry weight of *T. versicolor*, boxplot of cumulative particle distribution, experimental procedure for assessing surface roughness from SEM images, arithmetic mean roughness (Ra) of the substrate pellets, variability analysis on second derivative spectra, and average MIR spectra between 1100 and 1800 cm^{-1} (PDF)

AUTHOR INFORMATION

Corresponding Author

Arnaud Besserer − *Université de Lorraine, LERMaB, INRAe, Nancy F-54000, France*; Email: arnaud.besserer@univ-lorraine.fr

Authors

Laura Figel − *Université de Lorraine, LERMaB, INRAe, Nancy F-54000, France*; orcid.org/0009-0005-9041-5051

Kyle Aguilar − *Université de Lorraine, LERMaB, INRAe, Nancy F-54000, France; ADEME, Angers 49004, France*

Isabelle Ziegler-Devin − *Université de Lorraine, LERMaB, INRAe, Nancy F-54000, France*

Safwan Saker − *CRITT BOIS, Epinal 54500, France*

Nicolas Brosse − *Université de Lorraine, LERMaB, INRAe, Nancy F-54000, France*; orcid.org/0000-0001-8505-8401

Complete contact information is available at: https://pubs.acs.org/10.1021/acssuschemeng.5c00929

Author Contributions

#F.L. and A.K. contributed equally. The manuscript was written through contributions of all authors. All authors have given approval to the final version of the manuscript.

Notes

The authors declare no competing financial interest.

ACKNOWLEDGMENTS

This work is part of W2W Horizon Europe project. W2W is funded by the European Union (grant agreement ID: 101138789). Views and opinions expressed are, however, those of the authors only and do not necessarily reflect those of the European Union or HADEA. Neither the European Union nor the granting authority can be held responsible for them. The authors thank CF2P, Ecomaison, Lorraine Université d'Excellence (LUE), and ADEME (Agence de l'Environnement de la Maitrise de l'Energie) for the financial support in the PROFEX project. The authors thank the Platform Green Process for Wood (GP4Wood) of LERMaB (Université de Lorraine-INRAe), F-54000 Nancy, France. The authors thank Pierre-Jean Meausoone and Caroline Simon for providing the Camsizer. The authors thank Stéphane Aubert for help with the compression tests.

ABBREVIATIONS

ANOVA, analysis of variance; ATR-FTIR, attenuated total reflectance−Fourier transform infrared spectroscopy; DP, degree of polymerization; MIR, mid infrared; MIRS, mid infrared spectroscopy; NIR, near-infrared; NIRS, near-infrared spectroscopy; PCA, principal component analysis; SE, steam explosion; SEM, scanning electron microscopy

REFERENCES

(1) Kshirsagar, S. D.; Waghmare, P. R.; Chandrakant Loni, P.; Patil, S. A.; Govindwar, S. P. Dilute Acid Pretreatment of Rice Straw, Structural Characterization and Optimization of Enzymatic Hydrolysis Conditions by Response Surface Methodology. *RSC Adv.* **2015**, *5* (58), 46525−46533.

(2) Jain, S.; Kumar, S. Advances and challenges in pretreatment technologies for bioethanol production: A comprehensive review. *Sustainable Chemistry for Climate Action* **2024**, *5*, No. 100053.

(3) Kratky, L.; Azizov, S.; Jirout, T. Lignocellulosic Waste Treatment in Biogas Biorefinery with Reduced CO_2 Production: A Techno-Economic Study. *Chem. Eng. Trans.* **2018**, 1975.

(4) Hoang, A. T.; Nguyen, X. P.; Duong, X. Q.; Ağbulut, Ü.; Len, C.; Nguyen, P. Q. P.; Kchaou, M.; Chen, W.-H. Steam Explosion as Sustainable Biomass Pretreatment Technique for Biofuel Production: Characteristics and Challenges. *Bioresour. Technol.* **2023**, *385*, No. 129398.

(5) Ziegler-Devin, I.; Chrusciel, L.; Brosse, N. Steam explosion pretreatment of lignocellulosic biomass: a mini-review of theorical and experimental approaches. *Frontiers in Chemistry* **2021**, *9*, No. 705358.
(6) Roy, R.; Hewetson, B.; Schooff, B.; Bandi, S.; LaTour, P.; Iverson, B. D.; Fry, A. Steam explosion treated biomass as a renewable fuel source: A review from collection to combustion. *Fuel* **2024**, *378*, No. 132883.
(7) Kral, I.; Piringer, G.; Saylor, M. K.; Lizasoain, J.; Gronauer, A.; Bauer, A. Life Cycle Assessment of Biogas Production from Unused Grassland Biomass Pretreated by Steam Explosion Using a System Expansion Method. *Sustainability* **2020**, *12* (23), 9945.
(8) Elsacker, E.; Vandelook, S.; Van Wylick, A.; Ruytinx, J.; De Laet, L.; Peeters, E. A comprehensive framework for the production of mycelium-based lignocellulosic composites. *Science of The Total Environment* **2020**, *725*, No. 138431.
(9) Alemu, D.; Tafesse, M.; Mondal, A. K.; Seifalian, A. Mycelium-based composite: The future sustainable biomaterial. *Int. J. Biomater.* **2022**, *2022* (1), No. 8401528.
(10) Aiduang, W.; Jatuwong, K.; Jinanukul, P.; Suwannarach, N.; Kumla, J.; Thamjaree, W.; Teeraphantuvat, T.; Waroonkun, T.; Oranratmanee, R.; Lumyong, S. Sustainable Innovation: Fabrication and Characterization of Mycelium-Based Green Composites for Modern Interior Materials Using Agro-Industrial Wastes and Different Species of Fungi. *Polymers* **2024**, *16* (4), 550.
(11) Sydor, M.; Cofta, G.; Doczekalska, B.; Bonenberg, A. Fungi in Mycelium-Based Composites: Usage and Recommendations. *Materials* **2022**, *15* (18), 6283.
(12) Sun, W.; Tajvidi, M.; Hunt, C. G.; Cole, B. J. W.; Howell, C.; Gardner, D. J.; Wang, J. Fungal and enzymatic pretreatments in hot-pressed lignocellulosic bio-composites: A critical review. *J. Clean. Prod.* **2022**, *353*, No. 131659.
(13) Jo, W. S.; Kang, M. J.; Choi, S. Y.; Yoo, Y. B.; Seok, S. J.; Jung, H. Y. Culture conditions for mycelial growth of *Coriolus versicolor*. *Mycobiology* **2010**, *38* (3), 195−202.
(14) Aguilar, K.; Figel, L.; Saker, S.; Soufflet, L.; Brosse, N.; Besserer, A. Steam Explosion: A Booster for Fungal Growth in a Myco-Composite. *ACS Sustainable Chem. Eng.* **2024**, *12* (31), 11650−11659.
(15) Troilo, S.; Besserer, A.; Rose, C.; Saker, S.; Soufflet, L.; Brosse, N. Urea-Formaldehyde Resin Removal in Medium-Density Fiberboards by Steam Explosion: Developing Nondestructive Analytical Tools. *ACS Sustain. Chem. Eng.* **2023**, *11*, 3603.
(16) Overend, R. P.; Chornet, E. Fractionation of lignocellulosics by steam-aqueous pretreatments. *Philos. Trans. R. Soc., A* **1987**, *321* (1561), 523−536.
(17) Hanson, B. A.*ChemoSpec: An R Package for Chemometric Analysis of Spectroscopic Data* (Package Version 4.4.97).
(18) Sandak, A.; Sandak, J.; Zborowska, M.; Prądzyński, W. Near Infrared Spectroscopy as a Tool for Archaeological Wood Characterization. *J. Archaeol. Sci.* **2010**, *37* (9), 2093−2101.
(19) Qian, H.; Hou, Q.; Hong, L.; Lu, X.; Ziegler-Devin, I.; Chrusciel, L.; Besserer, A.; Brosse, N. Effect of Highly Efficient Steam Explosion Treatment on Beech, Poplar and Spruce Solid Wood Physicochemical and Permeable Performances. *Ind. Crops Prod.* **2022**, *182*, No. 114901.
(20) Langner, M.; Kitzmann, I.; Ruppert, A.-L.; Wittich, I.; Wolf, B. In-Line Particle Size Measurement and Process Influences on Rotary Fluidized Bed Agglomeration. *Powder Technol.* **2020**, *364*, 673−679.
(21) Brischke, C.; Alfredsen, G. Wood-Water Relationships and Their Role for Wood Susceptibility to Fungal Decay. *Appl. Microbiol. Biotechnol.* **2020**, *104* (9), 3781−3795.
(22) Besserer, A.; Mougnala Moukagni, E.; Ziegler-Devin, I.; Brosse, N. Extraction of Polymeric Hemicelluloses from Okoumé Sapwood by Steam Explosion: Use of Non-Destructive Characterization Methods. *Ind. Crops Prod.* **2024**, *208*, No. 117808.
(23) Takada, M.; Chandra, R. P.; Saddler, J. N. The Influence of Lignin Migration and Relocation during Steam Pretreatment on the Enzymatic Hydrolysis of Softwood and Corn Stover Biomass Substrates. *Biotechnol. Bioeng.* **2019**, *116* (11), 2864−2873.
(24) Skvaril, J.; Kyprianidis, K. G.; Dahlquist, E. Applications of Near-Infrared Spectroscopy (NIRS) in Biomass Energy Conversion Processes: A Review. *Appl. Spectrosc. Rev.* **2017**, *52* (8), 675−728.
(25) Besserer, A.; Obame, S. N.; Safou-Tchima, R.; Saker, S.; Ziegler-Devin, I.; Brosse, N. Biorefining of Aucoumea Klaineana Wood: Impact of Steam Explosion on the Composition and Ultrastructure the Cell Wall. *Ind. Crops Prod.* **2022**, *177*, No. 114432.
(26) Lancha, J. P.; Perré, P.; Colin, J.; Lv, P.; Ruscassier, N.; Almeida, G. Multiscale Investigation on the Chemical and Anatomical Changes of Lignocellulosic Biomass for Different Severities of Hydrothermal Treatment. *Sci. Rep.* **2021**, *11* (1), 8444.
(27) Kudahettige Nilsson, R. L.; Holmgren, M.; Madavi, B.; Nilsson, R. T.; Sellstedt, A. Adaptability of *Trametes versicolor* to the Lignocellulosic Inhibitors Furfural, HMF, Phenol and Levulinic Acid during Ethanol Fermentation. *Biomass Bioenergy* **2016**, *90*, 95−100.
(28) Op De Beeck, M.; Persson, P.; Tunlid, A. Fungal Extracellular Polymeric Substance Matrices − Highly Specialized Microenvironments That Allow Fungi to Control Soil Organic Matter Decomposition Reactions. *Soil Biol. Biochem.* **2021**, *159*, No. 108304.
(29) Morel-Rouhier, M.Wood as a Hostile Habitat for Ligninolytic Fungi. In *Advances in Botanical Research*; Elsevier, 2021; Vol. *99*, pp 115−149. DOI: .
(30) Nicole, M.; Chamberland, H.; Geiger, J. P.; Lecours, N.; Valero, J.; Rio, B.; Ouellette, G. B. Immunocytochemical Localization of Laccase L1 in Wood Decayed by Rigidoporus Lignosus. *Appl. Environ. Microbiol.* **1992**, *58* (5), 1727−1739.
(31) Ruel, K.; Joseleau, J.-P. Involvement of an Extracellular Glucan Sheath during Degradation of *Populus* Wood by *Phanerochaete Chrysosporium*. *Appl. Environ. Microbiol.* **1991**, *57* (2), 374−384.
(32) Op De Beeck, M.; Troein, C.; Siregar, S.; Gentile, L.; Abbondanza, G.; Peterson, C.; Persson, P.; Tunlid, A. Regulation of Fungal Decomposition at Single-Cell Level. *ISME J.* **2020**, *14* (4), 896−905.
(33) Barrasa, J. M.; Blanco, M. N.; Esteve-Raventós, F.; Altés, A.; Checa, J.; Martínez, A. T.; Ruiz-Dueñas, F. J. Wood and Humus Decay Strategies by White-Rot Basidiomycetes Correlate with Two Different Dye Decolorization and Enzyme Secretion Patterns on Agar Plates. *Fungal Genet. Biol.* **2014**.
(34) Hernando, A. V.; Sun, W.; Abitbol, T. "You Are What You Eat": How Fungal Adaptation Can Be Leveraged toward Myco-Material Properties. *Glob. Chall.* **2024**, *8*, No. 2300140.
(35) Jiang, L.; Walczyk, D.; McIntyre, G.; Bucinell, R.; Tudryn, G. Manufacturing of Biocomposite Sandwich Structures Using Mycelium-Bound Cores and Preforms. *J. Manuf. Process.* **2017**, *28*, 50−59.
(36) Aiduang, W.; Kumla, J.; Srinuanpan, S.; Thamjaree, W.; Lumyong, S.; Suwannarach, N. Mechanical, Physical, and Chemical Properties of Mycelium-Based Composites Produced from Various Lignocellulosic Residues and Fungal Species. *J. Fungi* **2022**, *8* (11), 1125.
(37) Zhang, M.; Zhang, Z.; Zhang, R.; Peng, Y.; Wang, M.; Cao, J. Lightweight, Thermal Insulation, Hydrophobic Mycelium Composites with Hierarchical Porous Structure: Design, Manufacture and Applications. *Compos. Part B Eng.* **2023**, *266*, No. 111003.
(38) Elsacker, E.; Vandelook, S.; Brancart, J.; Peeters, E.; De Laet, L. Mechanical, Physical and Chemical Characterisation of Mycelium-Based Composites with Different Types of Lignocellulosic Substrates. *PLoS One* **2019**, *14* (7), No. e0213954.

https://doi.org/10.1021/acssuschemeng.5c00929
ACS Sustainable Chem. Eng. XXXX, XXX, XXX−XXX